

DSMC Convergence Behavior for Transient Flows

M. A. Gallis¹, J. R. Torczynski², and D. J. Rader³

Engineering Sciences Center, Sandia National Laboratories, Albuquerque, New Mexico 87185-0826 USA

The convergence behavior of the Direct Simulation Monte Carlo (DSMC) method is investigated for transient flows. Two types of flows are considered: a Couette-like flow, in which an initial velocity profile decays in time, and a Fourier-like flow, in which an initial temperature profile decays in time. DSMC results are presented for hard-sphere argon with Knudsen numbers in the range 0.01-0.4. Low-Knudsen-number DSMC results are compared with Navier-Stokes results. The DSMC discretization errors from finite time step and finite cell size (in the limit of infinite number of computational molecules per cell) are compared with the predictions of Green-Kubo theory for conditions in this regime.

Nomenclature

c_0	= most probable molecular speed
D	= self-diffusion coefficient
d	= molecular diameter
k_B	= Boltzmann constant
Kn	= Knudsen number
K	= thermal conductivity
L	= distance between walls
m	= molecular mass
N_T	= total number of molecules used in simulation
n	= number density
p	= pressure
T	= temperature
ΔT	= amplitude of temperature variation
t	= time
t_0	= mean molecular collision time
Δt	= time step
u	= in-plane velocity component perpendicular to walls
v	= in-plane velocity component parallel to walls
Δv	= amplitude of velocity variation
w	= out-of-plane velocity component parallel to walls
x	= Cartesian coordinate perpendicular to walls
Δx	= cell size
λ	= molecular mean free path
μ	= absolute viscosity
ρ	= mass density
eff	= effective value
ref	= reference value
0	= initial or nominal value
DSMC	= Direct Simulation Monte Carlo
NS	= Navier-Stokes

¹ Technical Staff, Microscale Sciences and Technology Department, MS 0826, AIAA Member.

² Technical Staff, Microscale Sciences and Technology Department, MS 0826.

³ Manager, Microscale Sciences and Technology Department, MS 0826.

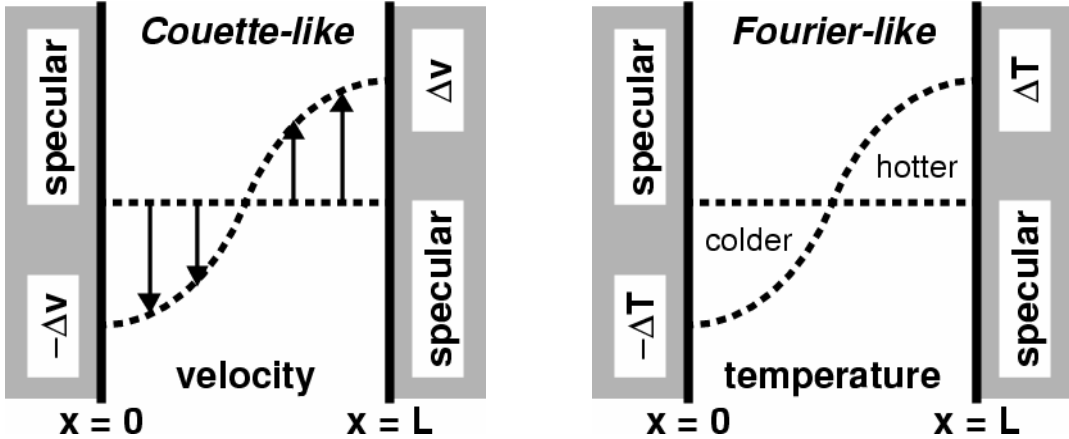


Figure 1. Left: shear-velocity-profile decay in Couette-like flow.
Right: temperature-profile decay in Fourier-like flow.

I. Introduction

The Direct Simulation Monte Carlo (DSMC) method of Bird is the most general and widely used method for simulating noncontinuum gas flows.¹ In this method, computational molecules move, reflect from solid boundaries, and collide with each other so as to statistically reproduce the behavior of real molecules. Steady DSMC simulations have been shown to yield solutions of the Boltzmann equation in the limit of vanishing discretization error.²⁻⁷ Moreover, the departures of DSMC simulations from such solutions have been shown to obey Green-Kubo theory for small but finite discretization errors (i.e., finite time step and cell size).⁸⁻¹¹ As a result, DSMC is often used as the standard by which other methods for simulating noncontinuum gas flows are assessed.¹²⁻¹⁵ In the last few years, various researchers have begun to apply DSMC to simulate transient flows.¹⁶⁻²⁰ However, there are few studies that systematically investigate the convergence behavior of DSMC for transient gas flows.²¹

In this paper, the convergence behavior of DSMC is investigated for transient gas flows. Two types of gas flows are considered (see Figure 1): a Couette-like flow, in which an initial cosine velocity profile decays in time, and a Fourier-like flow, in which an initial cosine temperature profile decays in time. In both cases, the gas is taken to be hard-sphere argon (i.e., argon with properties at STP taken from Bird¹ but with a hard-sphere collision interaction). The reason for this is to facilitate comparison with previous theoretical and numerical work.³⁻¹¹ The gas is confined between two parallel solid (impermeable) walls that are specularly reflecting. The reason for this choice of boundary condition is to be able to investigate the convergence of DSMC for transient flows without the additional complexity introduced by a more complicated interaction between the gas molecules and the solid boundary.

In the remaining sections, the following topics are covered. First, the theoretical results used in the present investigation are reviewed. These include Chapman-Enskog theory, Green-Kubo theory, and shear-flow decay. Second, DSMC simulations of Couette-like flow are presented and compared with Navier-Stokes (NS) simulations to determine the dependence of the effective viscosity on cell size and time step. The results of these simulations are compared to the predictions of Chapman-Enskog theory and Green-Kubo theory. Third, DSMC simulations of Fourier-like flow are presented and compared with NS simulations.

II. Theoretical Results

Chapman-Enskog theory predicts the viscosity, the thermal conductivity, the self-diffusion coefficient, and the Sonine-polynomial coefficients of the velocity distribution for a gas of identical hard-sphere molecules.³⁻⁷ The reference viscosity μ_{ref} at a reference temperature T_{ref} is related to the molecular mass m , the molecular diameter d_{ref} , the infinite-to-first-approximation viscosity ratio $\mu_{\infty}/\mu_1 = 1.016034$, and the Boltzmann constant k_B :³⁻⁷

$$\mu_{\text{ref}} = \frac{5(mk_B T_{\text{ref}})^{1/2}}{16\pi^{1/2} d_{\text{ref}}^2} \frac{\mu_{\infty}}{\mu_1}. \quad (1)$$

The viscosity μ , the thermal conductivity K , and the self-diffusion coefficient D of a hard-sphere gas all have a square-root temperature-dependence:³⁻⁵

$$\frac{\mu}{\mu_{\text{ref}}} = \frac{K}{K_{\text{ref}}} = \frac{D}{D_{\text{ref}}} = \left(\frac{T}{T_{\text{ref}}} \right)^{1/2}. \quad (2)$$

Green-Kubo theory provides expressions for the ratio of the effective viscosity μ_{eff} to the actual viscosity μ in terms of the cell size Δx and the time step Δt in a DSMC simulation. The following expressions for the mean free path λ , the mean collision time t_0 , and the most probable molecular speed c_0 are used:⁸⁻¹¹

$$\lambda = \frac{1}{2^{1/2} \pi d_{\text{ref}}^2 n}, \quad (3)$$

$$t_0 = \frac{\lambda}{c_0}, \quad (4)$$

$$c_0 = \left(\frac{2k_B T}{m} \right)^{1/2}. \quad (5)$$

For an ideal gas, the number density n and the mass density ρ are related to the pressure p , the temperature T , and the molecular mass m :

$$n = \frac{\rho}{m} = \frac{p}{k_B T}. \quad (6)$$

The Green-Kubo expression for the viscosity ratio is given below and is applicable in the limit of an essentially infinite number of molecules per cell, where the tildes denote dimensionless quantities:⁸⁻¹⁰

$$\frac{\mu_{\text{eff}}}{\mu} = 1 + \frac{16}{75\pi} \left(\frac{\Delta t}{t_0} \right)^2 + \frac{16}{45\pi} \left(\frac{\Delta x}{\lambda} \right)^2 = 1 + 0.0679 (\Delta \tilde{t})^2 + 0.1132 (\Delta \tilde{x})^2. \quad (7)$$

This expression is compared to the results of DSMC simulations in subsequent sections.

For the Couette-like flow in Figure 1 in the limit of small velocities ($\Delta v \ll c_0$) and small Knudsen numbers ($\text{Kn} = \lambda/L \ll 1$, where L is the distance between the walls), the Navier-Stokes (NS) equations have a closed-form solution for the velocity component v (in the y direction), where Δv is the amplitude of the initial cosine velocity profile:

$$v[x, t] = -\Delta v \cos \left[\frac{\pi x}{L} \right] \exp \left[-\frac{\pi^2 \mu t}{\rho L^2} \right]. \quad (8)$$

Under these conditions, all thermodynamic variables remain constant in time and uniform in space at their initial values, and the other two velocity components u and w (in the x and z directions, respectively, in Figure 1) remain equal to zero everywhere and for all time. With the replacement $\mu \rightarrow \mu_{\text{eff}}$, the above expression can be compared to the results of DSMC simulations to infer the effective viscosity. The above expression is applicable only in the limit that $\Delta v/c_0 \rightarrow 0$: at finite values of this ratio, the dissipated kinetic energy produces a small temperature rise and comparable perturbations in all other quantities (except w). Since all DSMC simulations are performed with finite values of $\Delta v/c_0$, using the above formula produces a small error in the effective viscosity thus determined. However, this error is extremely small for the conditions used in the following DSMC simulations.

III. Couette-like Transient Flow

Couette-like flow is shown in Figure 1. Initial conditions for the simulations are as follows. All thermodynamic quantities are uniform in space (i.e., in equilibrium), the gas velocity components u and w are zero everywhere, and the gas velocity component v initially varies according to $v[x, 0] = -\Delta v \cos[\pi x/L]$, where the region between the walls is $0 \leq x \leq L$. A uniform cell size of Δx is used throughout the domain, and constant time steps of Δt are taken. Table 1 shows the parameter values used in the simulations.¹

Table 1. Parameter values used in DSMC simulations.

Quantity	Symbol	Value or Range
Distance between walls	L	1 mm
Number of molecules, total	N_T	10^7
Cell size	Δx	2.5-25 μm (40-400 cells)
Time step	Δt	7-70 ns
Boltzmann constant	k_B	1.380658×10^{-23} J/K
Molecular mass	m	66.3×10^{-27} kg
Molecular diameter	d_{ref}	0.3658 nm
Temperature, reference	T_{ref}	273.15 K
Viscosity, reference	μ_{ref}	2.117×10^{-5} Pa·s
Thermal conductivity, reference	K_{ref}	0.01668 W/m·K
Temperature	T	273.15 K
Pressure	p	16.665-533.288 Pa
Number density	n	7.070×10^{22} m ⁻³ at 266.644 Pa
Mass density	ρ	4.688×10^{-3} kg/m ³ at 266.644 Pa
Most probable speed	c_0	337.3 m/s
Mean free path	λ	23.79 μm at 266.644 Pa
Mean collision time	t_0	70.54 ns at 266.644 Pa
Knudsen number	Kn	0.024 at 266.644 Pa
Velocity amplitude	Δv	50 m/s
Temperature amplitude	ΔT	50 K

Figure 2 shows velocity profiles from six DSMC simulations (points) and corresponding NS simulations (curves) with $\Delta v = 50$ m/s at Knudsen numbers of 0.38, 0.19, 0.095, 0.048, 0.024, and 0.012 (pressures of 16.665, 33.330, 66.661, 133.322, 266.644, and 533.288 Pa, respectively). The DSMC simulations are performed with a cell size of $\Delta x = 2.5 \mu\text{m}$ and a time step of $\Delta t = 7$ ns. At $p = 266.644$ Pa, these values correspond to dimensionless values of $\Delta \tilde{x} = 0.105$ and $\Delta \tilde{t} = 0.099$. The dimensionless values at other pressures are found using the fact that λ and t_0 are inversely proportional to the pressure. Thus, all DSMC results in this figure have dimensionless cell sizes and time steps around or well less than 0.2 and therefore represent highly resolved simulations.¹¹ The times at which the profiles are displayed are selected to show all stages of the decay. These times differ by a factor of two from one time to the next within each plot and by a factor of two from one plot to the next because the viscous decay time (proportional to $\rho L^2/\mu$ in the continuum limit) differs by a factor of two from one pressure to the next. The DSMC and NS profiles are virtually identical for $\text{Kn} \leq 0.024$, indicating that pressures of $p \geq 266.644$ Pa are large enough for continuum behavior to be obtained and for Equation (8) to be applicable.

Figure 3 shows velocity profiles from six DSMC simulations (points) and corresponding NS simulations (curves) at $p = 266.644$ Pa ($\text{Kn} = 0.024$) with DSMC cell sizes in the range $2.5 \mu\text{m} \leq \Delta x \leq 25 \mu\text{m}$ ($0.1 \leq \Delta \tilde{x} \leq 1$) and DSMC time steps in the range $7 \text{ ns} \leq \Delta t \leq 70 \text{ ns}$ ($0.1 \leq \Delta \tilde{t} \leq 1$). At the smallest cell size and time step, the DSMC profiles are virtually identical to the NS profiles, as indicated earlier. However, as the cell size and the time step are increased, the DSMC velocity profiles are observed to decay more rapidly than the NS velocity profiles. This indicates that the effective viscosity in the DSMC simulations increases as the cell size and the time step are increased, which is in accord with the predictions of Green-Kubo theory.

Figure 4 shows the DSMC velocity profiles (points) from the two coarsest simulations in the previous figure. The NS velocity profiles (curves) in this figure use effective viscosity values larger than the actual viscosity value, as indicated in the plot legends. The viscosity ratio is determined by adjusting the NS effective viscosity until the NS velocity profiles from Equation (8) match the corresponding DSMC velocity profiles most closely in a least-squares sense. The NS velocity profiles from simulations using these effective viscosity values are in very good agreement with the corresponding DSMC velocity profiles (unlike the NS velocity profiles from simulations using the actual viscosity). This type of comparison enables the effective viscosity in a DSMC simulation to be determined.

Figure 5 summarizes the results of 64 DSMC simulations for which the effective viscosity has been determined in the manner shown above. Four plots are included in this figure (all 64 DSMC values are present in all four plots). In the left two plots, the viscosity ratio is plotted against cell size with time step shown parametrically, whereas, in the right two plots, the viscosity ratio is plotted against time step with cell size shown parametrically. In the upper row of plots, the DSMC values are compared with the predictions of Green-Kubo theory, plotted as curves, whereas, in the lower row of plots, the DSMC values are shown with an empirically determined correlation:

$$\frac{\mu_{\text{eff}}}{\mu} = 0.9978 + 0.0670(\Delta \tilde{t})^2 + 0.0969(\Delta \tilde{x})^2 - 0.0209(\Delta \tilde{t})^2(\Delta \tilde{x})^2 + 0.0025(\Delta \tilde{t})^3(\Delta \tilde{x})^2. \quad (9)$$

As the cell size and the time step become small, the DSMC viscosity ratio approaches 0.9978. This value is close to unity, indicating that high-resolution transient DSMC simulations reproduce the Chapman-Enskog viscosity. The difference from unity is attributed to the fact that the conversion of the kinetic energy of the initial velocity profile into heat produces a temperature rise of 2 K with a corresponding increase in the actual viscosity of 0.003 (0.3%). Since this quantity is in the denominator of Equation (9), an increase of 0.003 decreases the viscosity ratio by 0.003, which is very close to the observed decrease below unity. The DSMC values are in reasonable agreement with but always slightly smaller than the Green-Kubo values. The DSMC and Green-Kubo coefficients of the $(\Delta \tilde{t})^2$ term are essentially identical, whereas the DSMC coefficient of the $(\Delta \tilde{x})^2$ term is about 14% smaller than the Green-Kubo coefficient of this term. This level of agreement is similar to what is observed for steady flows.¹¹

IV. Fourier-like Transient Flow

Fourier-like flow is shown in Figure 1. Initial conditions for the simulations are as follows. The temperature varies according to $T[x, 0] = T_0 - \Delta T \cos[\pi x/L]$, the mass density varies so as to yield a spatially uniform pressure, and all velocity components are zero everywhere. As before, a uniform cell size of Δx is used throughout the domain, and constant time steps of Δt are taken. Table 1 shows the parameter values used in the simulations.¹

Figure 6 shows temperature profiles from six DSMC simulations (points) and corresponding NS simulations (curves) with $\Delta T = 50$ K at the same Knudsen numbers, pressures, cell sizes, and time steps considered in Figure 2. In accord with observations for Couette-like flow, the DSMC and NS temperature profiles for Fourier-like flow are virtually identical for $\text{Kn} \leq 0.024$, indicating that pressures of $p \geq 266.644$ Pa are large enough for continuum behavior to be obtained. However, the temperature differences used in these simulations are too large for a small-amplitude expression like Equation (8) but for temperature to be accurate. While full NS simulations using effective properties could in principle be compared to DSMC profiles, effective values for both the thermal conductivity and the viscosity would have to be used since the solution depends on both transport properties. Because of the increased complexity that this involves, this has not been done at present. However, the excellent agreement between transient DSMC and NS temperature profiles for continuum conditions is noted, including the fact that the spatially uniform temperature value at long times is less than the initial value. This phenomenon is related to the above initial condition, which, with a spatially uniform pressure, has more “cold” molecules than “hot” molecules: the average energy corresponds to a (final) temperature slightly less than T_0 .

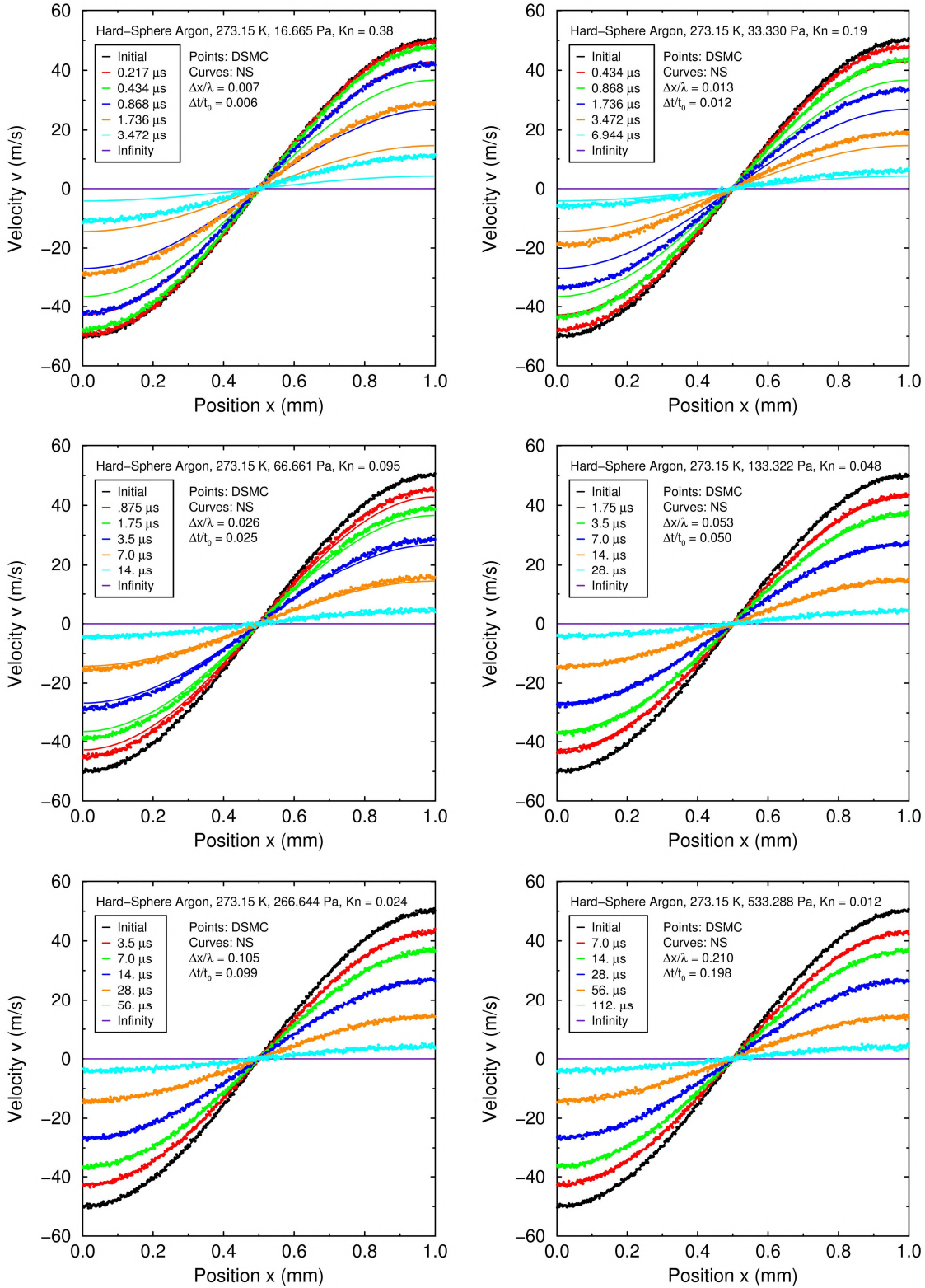


Figure 2. Transientsly decaying velocity profiles at six pressures.

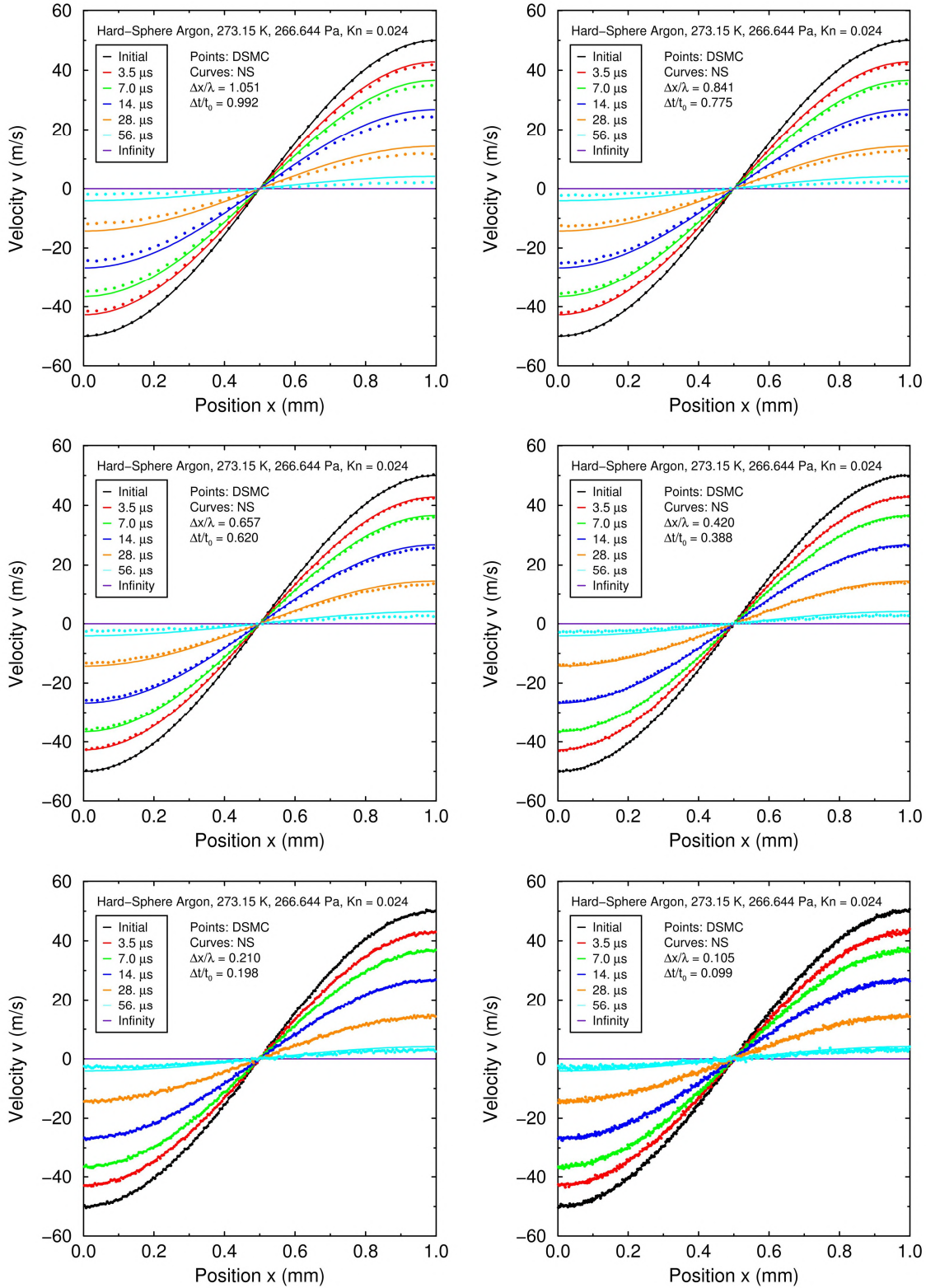


Figure 3. Transiently decaying velocity profiles at six combinations of cell size and time step.

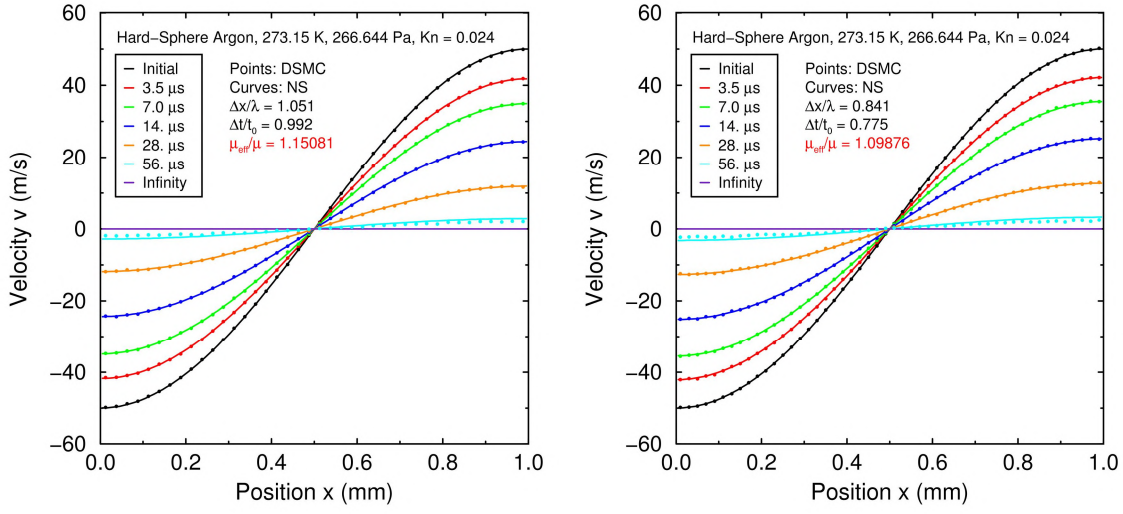


Figure 4. Transiently decaying velocity profiles with effective viscosity in NS.

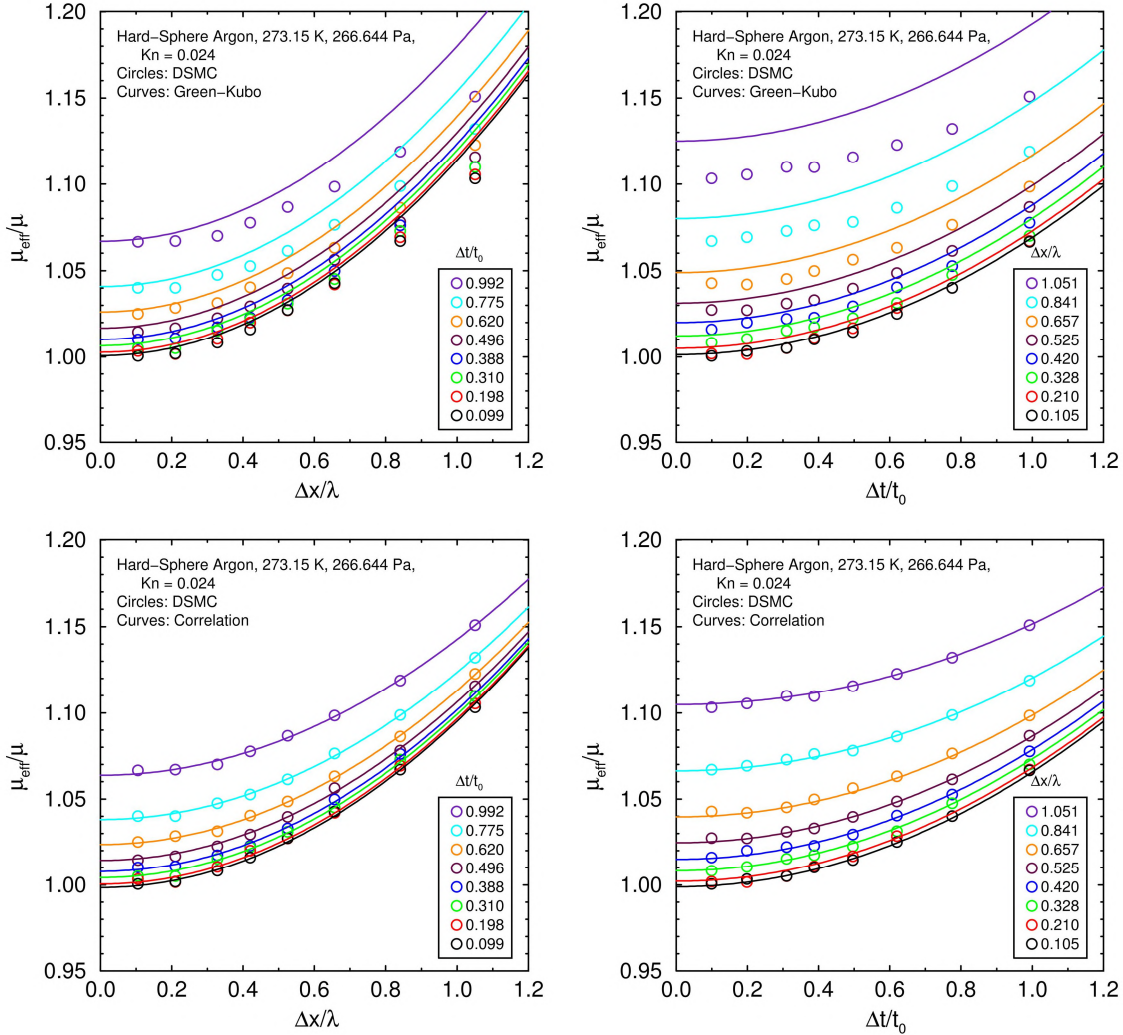


Figure 5. Effect of cell size and time step on effective viscosity from DSMC simulations: upper row, DSMC and Green-Kubo theory; lower row, DSMC and correlation.

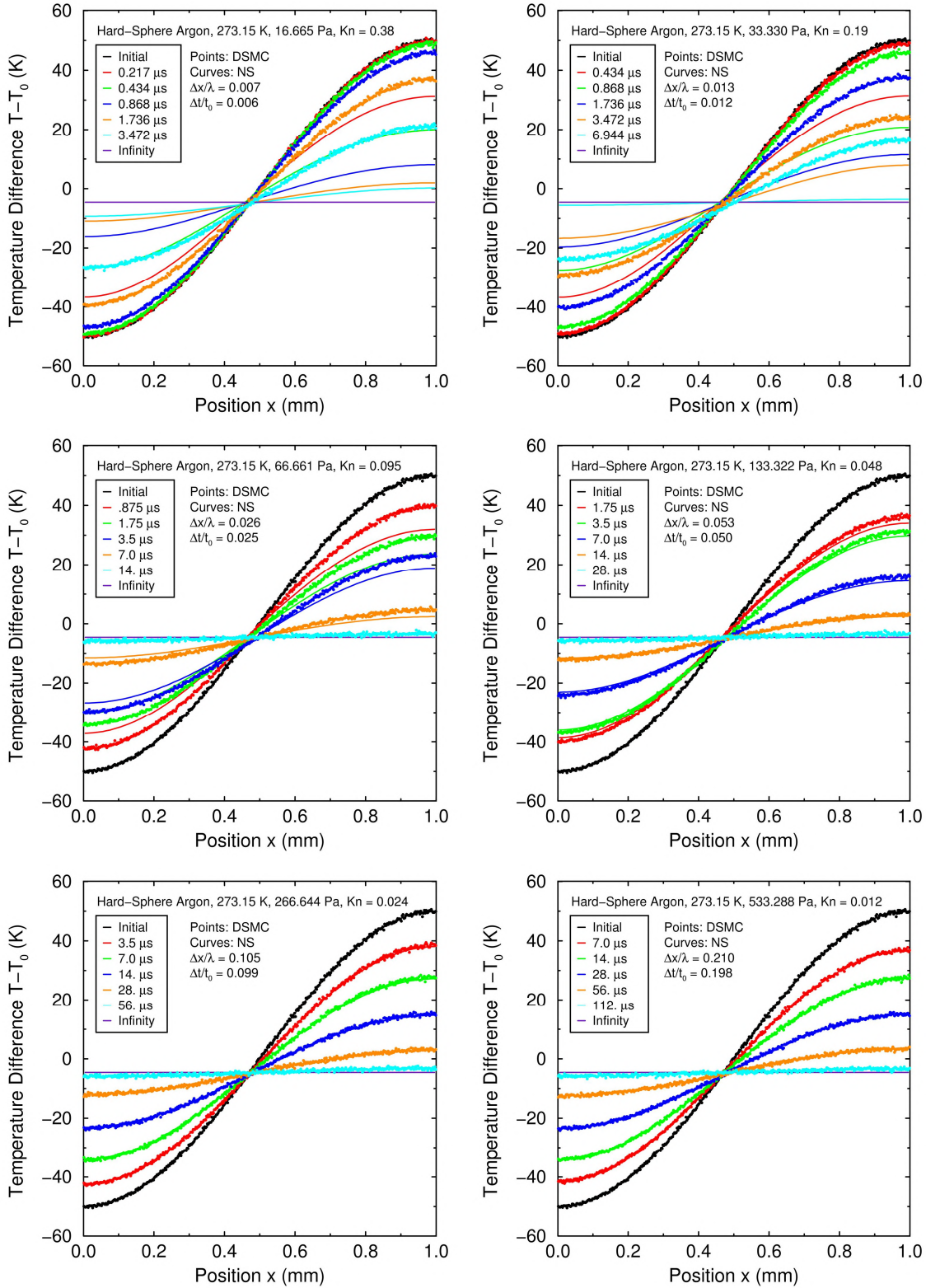


Figure 6. Transiently decaying temperature profiles at six pressures.

V. Conclusions

Transient DSMC and NS simulations of Couette-like and Fourier-like flows are compared. At pressures high enough to achieve continuum behavior (here, for $\text{Kn} \leq 0.024$), excellent agreement is observed. For Couette-like flow, the effective viscosity in a DSMC simulation is determined by comparison to NS simulations. The dependence of the DSMC effective viscosity on the cell size and the time step are determined in this manner and found to agree reasonably well with the predictions of Green-Kubo theory. These results provide strong evidence that DSMC provides accurate simulations of transient flows and that Green-Kubo theory provides a reasonable estimate of the cell-size and time-step errors for transient, as well as steady, flows.

Acknowledgments

This work was performed at Sandia National Laboratories. Sandia is a multiprogram laboratory operated by Sandia Corporation, a Lockheed Martin Company, for the United States Department of Energy's National Nuclear Security Administration under contract DE-AC04-94AL85000.

References

- ¹ Bird, G. A., *Molecular Gas Dynamics and the Direct Simulation of Gas Flows*, Clarendon Press, Oxford, UK, 1994, as updated in 1998.
- ² Wagner, W., "A Convergence Proof for Bird's Direct Simulation Monte Carlo Method for the Boltzmann Equation," *Journal of Statistical Physics*, Vol. 66, Nos. 3/4, 1992, pp. 1011-1044.
- ³ Pekeris, C. L., "Solution of the Boltzmann-Hilbert Integral Equation," *Proceedings of the National Academy of Science of the USA*, Vol. 41, 1955, pp. 661-669.
- ⁴ Pekeris, C. L., and Alterman, Z., "Solution of the Boltzmann-Hilbert Integral Equation II. The Coefficients of Viscosity and Heat Conduction," *Proceedings of the National Academy of Science of the USA*, Vol. 43, 1957, pp. 998-1007.
- ⁵ Chapman, S., and Cowling, T. G., *The Mathematical Theory of Non-Uniform Gases*, third edition, Cambridge University Press, Cambridge, UK, 1970.
- ⁶ Gallis, M. A., Torczynski, J. R., and Rader, D. J., "Molecular Gas Dynamics Observations of Chapman-Enskog Behavior and Departures Therefrom in Nonequilibrium Gases," *Physical Review E*, Vol. 69, No. 4, 2004, paper 042201, pp. 1-4.
- ⁷ Gallis, M. A., Torczynski, J. R., Rader, D. J., Tij, M., and Santos, A., "Normal Solutions of the Boltzmann Equation for Highly Nonequilibrium Fourier and Couette Flow," *Physics of Fluids*, Vol. 18, No. 1, 2006, paper 017104, pp. 1-15.
- ⁸ Alexander, F. J., Garcia, A. L., and Alder, B. A., "Cell Size Dependence of Transport Coefficients in Stochastic Particle Algorithms," *Physics of Fluids*, Vol. 10, No. 6, 1998, pp. 1540-1542; "Erratum: 'Cell Size Dependence of Transport Coefficients in Stochastic Particle Algorithms' [Phys. Fluids 10, 1540 (1998)]," *Physics of Fluids*, Vol. 12, No. 3, 2000, p. 731.
- ⁹ Garcia, A. L., and Wagner, W., "Time Step Error in Direct Simulation Monte Carlo," *Physics of Fluids*, Vol. 12, No. 10, 2000, pp. 2621-2633.
- ¹⁰ Hadjiconstantinou, N. G., "Analysis of Discretization in the Direct Simulation Monte Carlo," *Physics of Fluids*, Vol. 12, No. 10, 2000, pp. 2634-2638.
- ¹¹ Rader, D. J., Gallis, M. A., Torczynski, J. R., and Wagner, W., "DSMC Convergence Behavior of the Hard-Sphere-Gas Thermal Conductivity for Fourier Heat Flow," *Physics of Fluids*, Vol. 18, No. 7, 2006, paper 077102, pp. 1-16.
- ¹² Karniadakis, G. E., and Beskok, A., *Micro Flows: Fundamentals and Simulation*, Springer-Verlag, New York, NY, 2002.
- ¹³ Karniadakis, G., Beskok, A., and Aluru, N., *Microflows and Nanoflows: Fundamentals and Simulation*, Springer, New York, NY, 2005.
- ¹⁴ Liou, W. W., and Fang, Y., *Microfluid Mechanics: Principles and Modeling*, McGraw-Hill, New York, NY, 2006.
- ¹⁵ Gad-el-Hak, M. (editor), *MEMS: Introduction and Fundamentals*, Taylor & Francis, Boca Raton, FL, 2006.
- ¹⁶ Stefanov, S., Gospodinov, P., and Cercignani, C., "Monte Carlo Simulation and Navier-Stokes Finite Difference Calculation of Unsteady-State Rarefied Gas Flows," *Physics of Fluids*, Vol. 10, No. 1, 1998, pp. 289-300.
- ¹⁷ Park, J. H., Baek, S. W., Kang, S. J., and Yu, M. J., "Analysis of Thermal Slip in Oscillating Rarefied Flow," *Numerical Heat Transfer, Part A*, Vol. 42, 2002, pp. 647-659.
- ¹⁸ Park, J. H., Bahukudumbi, P., and Beskok, A., "Rarefaction Effects on Shear Driven Oscillatory Gas Flows: A Direct Simulation Monte Carlo Study in the Entire Knudsen Regime," *Physics of Fluids*, Vol. 16, No. 2, 2004, pp. 317-330.
- ¹⁹ Baker, L. L., and Hadjiconstantinou, N. G., "Variance Reduction for Monte Carlo Solutions of the Boltzmann Equation," *Physics of Fluids*, Vol. 17, No. 5, 2005, paper 051703, pp. 1-4.
- ²⁰ Gallis, M. A., Torczynski, J. R., and Rader, D. J., "DSMC Simulations of Transient Microbeam Gas Flow," *Bulletin of the American Physical Society*, Vol. 49, No. 9, 2004, p. 90.
- ²¹ Hokazono, T., Kobayashi, S., Ohsawa, T., and Ohwada, T., "On the Time Step Error of the DSMC," *Rarefied Gas Dynamics: 23rd International Symposium*, edited by A. D. Ketsdever and E. P. Muntz, American Institute of Physics, Melville, NY, 2003, pp. 390-397.